Safety assessment of unmanned aerial vehicle operations in an integrated airspace

Yazdi Ibrahim Jenie, Y; van Kampen, EJ; Ellerbroek, J; Hoekstra, JM

DOI
10.2514/6.2016-1000

Publication date
2016

Document Version
Accepted author manuscript

Published in
Proceedings of the AIAA infotech at aerospace

Safety Assessment of Unmanned Aerial Vehicle Operations in an Integrated Airspace

Yazdi I. Jenie* Erik-Jan van Kampen† Joost Ellerbroek‡ Jacco M. Hoekstra§

Control and Simulation Section, Faculty of Aerospace Engineering, Delft University of Technology

This paper focuses on the safety assessment of Unmanned Aerial Vehicles (UAVs) operating in an integrated airspace system. The assessment is based on series of Monte Carlo Simulations to include the effect of the variety of Conflict Detection and Resolution (CD&R) systems in each involved vehicle. The difficulty of using Monte Carlo simulations in the assessment, in which collision are rare to be sufficiently represented, is overcome by the use of a high density airspace with a periodic boundary condition. This setup, along with the randomization of the UAV states and the CD&R parameters, increases the number of conflicts and resolutions for each Monte Carlo sample to rapidly reach convergence. The parameters derived, including the mean ratio of time in which the vehicle are in either mission mode, avoidance mode, or in a Near Mid Air Collision (NMAC) situation, are compared to similar Monte Carlo simulation results where no CD&R system is used. The proposed method is a versatile safety assessment method for various encounter situations a UAV an its CD&R system might face in its operation in an integrated airspace system.

Nomenclature

$\bar{\tau}^{\mathrm{NMAC}}$	mean ratios of NMAC, [-]
$\bar{\tau}^{av}$	mean ratios of avoidance time, [-]
$\bar{\tau}^{ma}$	mean ratios of maintain time, [-]
$\bar{\tau}^{mi}$	mean ratios of mission time, [-]
χ_i	Heading of vehicle-i, [-]
ϵ_i	Error in obstacle position detection, [m]
ϵ_i	Error in obstacle velocity detection, [m/s]
ψ_i	Obstacle position azimuth angle, [-]
ρ_{int}	Density of an Area of Interest, $[-/m^2]$
A_{int}	Area of interest, $[m^2]$
d_{avo}	Preferred avoidance distances, [m]
D_i	Distance of vehicle-i, [m]
DIV	Velocity-Obstacle set of obstacle-i, [m/s]
L_x, L_y	Length of A_{int} edges, [m]
N_v	Number of involved vehicles, [-]
N_{MC}	Number of Monte Carlo simulation samples, [-]
r_{NMAC}	Radius of the Near Mid-Air collision zone, [m]
r_{sep}	Preferred separation radii, [m]
V_{avo}	Avoidance velocity, [m/s]
V_i	Speeds of vehicle-i, [m/s]
VO	Velocity-Obstacle set of obstacle-i, [m/s]
X_i	Global Position of vehicle-i, [m]

*PhD Student, Faculty of Aerospace Engineering, Delft University of Technology, 2629HS, Delft, The Netherlands
†Assistant Professor, Faculty of Aerospace Engineering, Delft University of Technology, 2629HS, Delft, The Netherlands
‡Assistant Professor, Faculty of Aerospace Engineering, Delft University of Technology, 2629HS, Delft, The Netherlands
§Professor, Faculty of Aerospace Engineering, Delft University of Technology, 2629HS, Delft, The Netherlands

This is a self-archived version. Please find the completed version of this paper at http://arc.aiaa.org/doi/10.2514/6.2016-1000 (doi:10.2514/6.2016-1000)

I. Introduction

Integrating Unmanned Aerial Vehicles (UAVs) into the current air traffic presents new challenges for the airspace management, especially in ensuring their operational safety. With the potentially large number of developers, operators, and missions, the vast variation of methods in UAV Conflict Detection and Resolution (CD&R) system is inevitable, which would create a heterogeneous environment for operation. This becomes a problem since most of the CD&R systems are yet to be proven in handling such heterogeneous situations, in the integrated airspace. On the other hand, subjected to a standardized CD&R procedures in manned-flight, both airspace authorities and regulations cannot yet accommodate the heterogeneousness as well. Taking safe measures, current policy to enable the integration of UAVs in the airspace is to define a target level of safety (TLOS), as it is stated in 1. One parameter of the target level of safety is the probability of Near Mid-Air Collision (NMAC). If strictly taken, the TLOS for NMAC probability for a UAV in an airspace should be less than one collision out of a billion operations (10^{-9}).

While many methods have been proposed to analytically asses the operational level of safety, most of them do not include the effects of the CD&R system in their calculation, let alone a variation in the system. Ref. 2 and 3, for instance, introduce the derivation of risk of collision as the expected number of collisions over a specified period of time, assuming constant velocities of the vehicle. Using the same assumption, Ref. 4 introduce a gas model for two and three body representations, making calculations based on a homogeneous distribution of aircraft in several different density assumptions. Most of these studies define uncertainties in the vehicle positions and velocities in the NMAC probability derivations.

Including the CD&R factor in a safety assessment is in fact difficult without an extensive method of modeling and simulation of the vehicle dynamics, such as by performing Monte Carlo simulations,[5] or by using dynamic programming.[6] With these methods, random samples can be inserted to model the variation of the UAV CD&R system and initial states in an airspace. Repeated simulation is then conducted across the samples that generates various conflict encounters and resolutions, and in the end draws out required parameters for safety assessment. These methods, however, are rarely desirable for safety analysis, especially when estimating the probability of collisions, since, in a realistic airspace density, collisions are very rare that it will take a considerably large amount of time and samples to obtain a sufficient result. Most of the time, the samples will result in zero collision occurrence, such as presented in 7 and 8 .

The current paper presents a method of safety assessment for UAV operations in an integrated airspace by resorting to the Monte Carlo simulations. To overcome the drawbacks of the method, a high density airspace is modeled, where a hundred UAVs are initiated, positioned close together in an upright square-lattice with random headings and speeds. The heterogeneousness of the air traffic is modeled in two elements, i.e., the uncertainties of detection and the variation of conflict resolutions. The density of the airspace is maintained using a Periodic Boundary Condition. This setup wraps the movement of vehicles inside the area of interest, eliminating the unavailing samples of the Monte Carlo simulations, such as, for example, vehicles that leave the area of interest before having chance to encounter a conflict.

The simulation setup will make the Monte Carlo process reaches convergence faster with the increase the chances for each vehicle to encounter, and therefore resolve, conflicts. Furthermore, since the safety parameter is averaged for the vehicles, each of the airspace samples already have one hundred samples of random conflicts and avoidances, which in the end speeds up the parameter convergence even more.

This paper is structured as follows. After this introduction, Section II discusses the heterogeneous air traffic model, which consists of three main elements, i.e. (1) the high density airspace, (2) the uncertainties of detection, and (3) the variety of resolutions. Section III presents the result of the Monte Carlo simulation based on that model. Results of the simulations where no CD&R is involved are also presented for comparison, along with a brief discussion.Section V concludes the paper and provides suggestions for future work.

II. Heterogeneous Airspace Model

A simulator capable of simulating up to a hundred independent vehicles is built using MATLAB, where each of the vehicles can have different own error in detection and preferences in the conflict resolution. The simulator run on discrete time step and models the involved vehicles as point masses, neglecting their control and dynamics. Instead, the simulator focuses more on the CD&R system in a randomized environment. Furthermore, in this paper, only two-dimensional encounter case are analyzed in this preliminary assessment

This is a self-archived version. Please find the completed version of this paper at http://arc.aiaa.org/doi/10.2514/6.2016-1000 (doi:10.2514/6.2016-1000)

Table 1. parameter randomization ranges

Parameters	Range	Unit
Initial positions†, $X(x_g, y_g)$	$(-\frac{1}{2}L_{x,y}, \frac{1}{2}L_{x,y})$	[m]
Initial headings, χ_g	$(0, 2\pi)$	[-]
Error in Detection of:		
Obstacle Positions, ϵ_X	$(-2, 2)$	[m]
Obstacle Velocities, ϵ_V	$(-0.5, 0.5)$	[m/s]
Parameter of Conflict Resolutions:		
Avoidance Distance, d_{avo}	$(r_{\mathrm{NMAC}}, 4r_{\mathrm{NMAC}})$,	[m]
Separation Radius, r_{sep}	$(\frac{1}{2}r_{\mathrm{NMAC}}, 2r_{\mathrm{NMAC}})$	[m]

† Not randomized.

of the CD&R architecture. The 3D part, however, is a case that is less stressful than the 2-Dimension, since the vehicles can exploit more space in order to reach safety.

Three key elements of the simulator, to represent the work of heterogeneous CD&R system in an integrated airspace, are explained in this section, which includes the airspace representation, the uncertainty in detection, the variety of resolution. These elements are also the source of collisions and is designed to produce as many collisions as possible in order to reduce the Monte Carlo sample requirement while maintaining the rationale. Table 1 lists the parameter randomization for the Monte Carlo simulations, which is explained in the following subsections.

A. High Density Airspace with Periodic Boundary Condition

The research initialized vehicles in a high density airspace setup, where one hundred UAVs are packed symmetrically in a square area of interest, in a upright square-lattice configuration, as shown in Figure1-a. This setup effectively generates more conflicts among the vehicles and creates many chances to test the CD&R system.

The initial distances of the vehicles with each of its four orthogonal neighbors are 200 meters, 300 meters, and 400 meters, which produce three values of airspace density, i.e., $25/km^2$, $11.11/km^2$, and $6.25/km^2$, respectively. as presented in Table 1. The area of interest dimensions therefore are $L_x = L_y = 2000$, 3000, and 4000 meters. The headings χ_i of each vehicle are uniformly randomized, from 0 to 360 degree from the North. This produces various encounter situations required for the Monte Carlo analysis, even if the initial positions of each vehicle are arranged in square-lattice configuration.

The simulation is conducted within a square boundary without any physical walls, where the density parameter is maintained by resorting to two-dimensional Periodic Boundary Condition (PBC) , as shown in Figure1-b. This boundary condition assumes that the area of interest is a unit cell, that is part of a large (infinite) uniform system. Thus, as presented in equation (1) and (2), whenever a vehicle crosses one of the edge of the area of interest, it gets wrapped on the opposite edge, while conserving the corresponding velocity vector. This setup also eliminates unavailing cases where some vehicles directly leave the area of interest without having chance to perform any avoidance, due to the random heading initialization.

$$\vec{X}(k+1) = \vec{X}(k) + \vec{V}(k)\Delta t + \begin{bmatrix} \sigma_x & 0 \\ 0 & \sigma_y \end{bmatrix} \begin{bmatrix} L_x \\ L_y \end{bmatrix} \tag{1}$$

where

$$\begin{cases} \sigma_x = -1, & \text{if} \quad (x(k) + v_x(k)\Delta t) > \frac{1}{2}L_x \\ \sigma_x = 1, & \text{if} \quad (x(k) + v_x(k)\Delta t) < -\frac{1}{2}L_x \\ \sigma_x = 0, & \text{otherwise} \end{cases}, \qquad \begin{cases} \sigma_y = -1, & \text{if} \quad (y(k) + v_y(k)\Delta t) > \frac{1}{2}L_y \\ \sigma_y = 1, & \text{if} \quad (y(k) + v_y(k)\Delta t) < -\frac{1}{2}L_y \\ \sigma_y = 0, & \text{otherwise} \end{cases} \tag{2}$$

This is a self-archived version. Please find the completed version of this paper at http://arc.aiaa.org/doi/10.2514/6.2016-1000 (doi:10.2514/6.2016-1000)

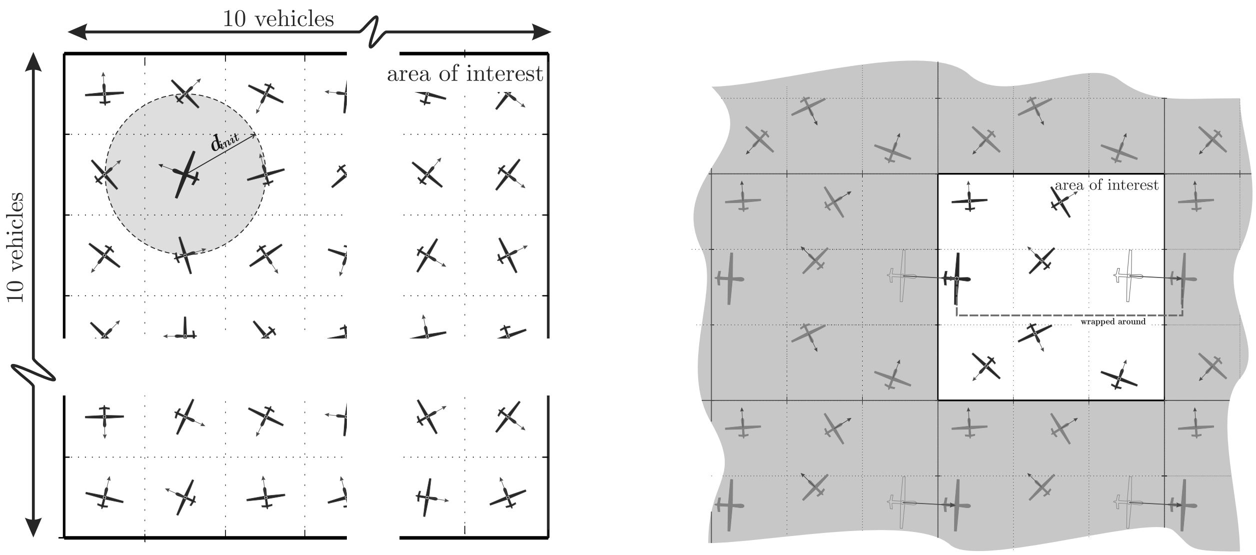

(a)

(b)

Figure 1. (a) initial setup of the airspace with 100 vehicles arranged in a square lattice; (b) The Wrap-around effect of the Periodic Boundary Condition applied in the airspace

In implementing the PBC, the wrap-around effect need to be considered in the conflict detection and resolution generation. This is illustrate in Figure 1-b, where vehicle B need to avoid C, which position is actually far away from B on the upper left corner of the area. Therefore, the 'clones' of vehicles near to the edges should be considered in the Velocity Obstacle resolutions.

In cases where body-to-body collision occurred due to failure in avoidance, the density of the area cannot be maintaine, since all involved vehicles are removed immediately. Although this setup might make some of the Monte Carlo simulation samples unavailing, the chances of body-to-body collision should be very small if the heterogeneous CD&R performs well. Loss of separations, on the other hand, does not remove the involved vehicles from the simulation, and therefore the vehicles might face loss of separation more than once.

B. The Uncertainty of Conflict Detection

The whole CD&R process begin with detection of obstacles in proximity, and whether of not the obstacle is in a conflicting course with the ownship. At least two state are required for this determination, that is, position and velocity vectors of all the involved vehicles. These can be obtained using the flight data exchange (dependent surveillance such as ADS-B information), or by on-board sensor the measurement (independent surveillance such as camera system). Since on-board sensors give an indirect data by series of calculation from, for example, distance and bearing measurements, this paper assumed that the states are obtained directly by data exchange for simplicity.

The uncertainty of detection is therefore represented by adding a specified errors on the position and velocity vector measurements of the obstacle in proximity by each vehicles. In two dimensional space, both vectors consist the X and Y with respect to the ownship flight course (wind-axis). Since the base of surveillance is the data exchanges, the errors is represented as a random error which is not affected by the states itself, and instead they are represented by a uniform error through time.

The range of error in the position vector is chosen to be well inside the Navigational Accuracy Category for Position and Velocity of NACp-11 and NACv-3, corresponding to the ADS-B requirements presented in.[9] Although measurement error should also be randomized across the vehicles, in this research it is only applied each time step, which mean that each vehicle have the same probability of errors in term of their means and variance. On the overall result, it is found that error probability difference between vehicles are negligible compare to the variety of resolution preferences.

This is a self-archived version. Please find the completed version of this paper at http://arc.aiaa.org/doi/10.2514/6.2016-1000 (doi:10.2514/6.2016-1000)

$$\vec{D}_i^* = \begin{bmatrix} x_i^* \\ y_i^* \end{bmatrix} = \begin{bmatrix} x_i + \epsilon_x \\ y_i + \epsilon_x \end{bmatrix} \tag{3}$$

$$\vec{V}_i^* = \begin{bmatrix} v_{i_x}^* \\ v_{i_y}^* \end{bmatrix} = \begin{bmatrix} v_{i_x} + \epsilon_v \\ v_{i_y} + \epsilon_v \end{bmatrix} \tag{4}$$

C. The Variation of Conflict Resolution

A vast collection conflict resolution algorithm can be found in the literature, many of them are reviewed and classified in Ref. 10 and 11. Unlike in manned flight, it is presumably difficult to regulate a single algorithm for all UAVs with their variation of mission, and their less complicated development cost and time. Therefore, to better assess the safety of UAV operation in an integrated airspace, a heterogeneous situation should be assumed. The assumption also required to have a better measurement on a resolution algorithm performance.

To represent the variety of resolutions, this research use the Velocity Obstacle method (VO-method)[8,12] as the basis. The method can produce variety of resolution by changing two of its variables, the avoidance distance, and the separation radius, as it will be detailed in the following paragraph. The variety of preferences, therefore, can be produced by randomization of those two parameters across the vehicles in one Monte Carlo sample, as well as across the samples. This scheme, however, will only cover a reactive avoidance, where a resolution is prescribed based on the instantaneous geometry of an encounter without any predetermined plan or any dynamic predictions.

The concept of the VO-method can be explained using Figure 2. For every encounter case, a collision cone can be drawn, in which every relative velocity vectors of the ownship that intersect a specified separation zone (S_{sep}) are collected. The protected zone is a threshold area around the obstacle that should be avoided, and therefore every intersecting relative velocity will eventually lead to a violation in the future. The VO-method use its absolute velocity vector representation of the CC set, the VO set, as depicted in the Figure 2-b, by translating the CC along the obstacle velocity. Hence, to avoid violating the S_{sep}, the ownship need to change and maintain its velocity vector to any reachable point outside the VO set before the violation, e.g., by a pure turning to one of the V_{avo} on the VO set edges. The ownship, therefore, changes its mode as shown in Figure 2: to mission mode where it head to its original goal, to avoid mode where it turn to one of the V_{avo}, and maintain mode where it keep its current velocity.

Equation (5) to (7) can be used to determined the Vo inclusion in the VO set after the conflict is imminent, i.e., the distance between the two vehicles d_{oi} is smaller than a specified avoidance starting point d_{avo}.

$$\vec{V}_o = \begin{bmatrix} v_{o_x} \\ v_{o_y} \end{bmatrix} \qquad \vec{D}_i^* = \begin{bmatrix} x_i^* \\ y_i^* \end{bmatrix} \qquad \vec{V}_i^* = \begin{bmatrix} v_{i_x}^* \\ v_{i_y}^* \end{bmatrix} \tag{5}$$

$$\psi_i = \arctan\left(\frac{y_i^*}{x_i^*}\right) \qquad \chi_i = \arctan\left(\frac{v_{i_y}^*}{v_{i_x}^*}\right) \qquad \alpha_{vo} = \arccos\left(\frac{\sqrt{\left|\vec{D}_i^*\right|^2 - r_{pz}^2}}{\left|\vec{D}_i^*\right|}\right) \tag{6}$$

$$\vec{V}_o \in \mathbf{VO}_i \iff \left\{ 0 < \frac{\left[\vec{V}_o - \vec{V}_i^*\right] \cdot \vec{D}_i^*}{\left|\vec{V}_o - \vec{V}_i^*\right| \left|\vec{D}_i^*\right|} < \cos\alpha_{vo} \quad \wedge \quad \left|\vec{D}_i^*\right| < d_{avo} \right\} \tag{7}$$

The avoidance velocity vectors $V_{avo} = \left(v_{avo_x}, v_{avo_y}\right)$ for both direction can be derived geometrically, by the intersection of the ownship reachable velocity circle with both edge of the VO. There will be four set of solutions that should satisfied system of linear and quadratic equation presented in equation (8) to (10), which are functions of d_{avo} and the radius of the separation zone r_{sep}, in a particular obstacle bearing (ψ_{oi}) and velocity of the vehicles ($\vec{V}_o$ and $\vec{V}_i$).

$$v_{a_y} + m_{vo} v_{a_x} = v_{i_y}^* + m_{vo} v_{i_x}^* \tag{8}$$

This is a self-archived version. Please find the completed version of this paper at http://arc.aiaa.org/doi/10.2514/6.2016-1000 (doi:10.2514/6.2016-1000)

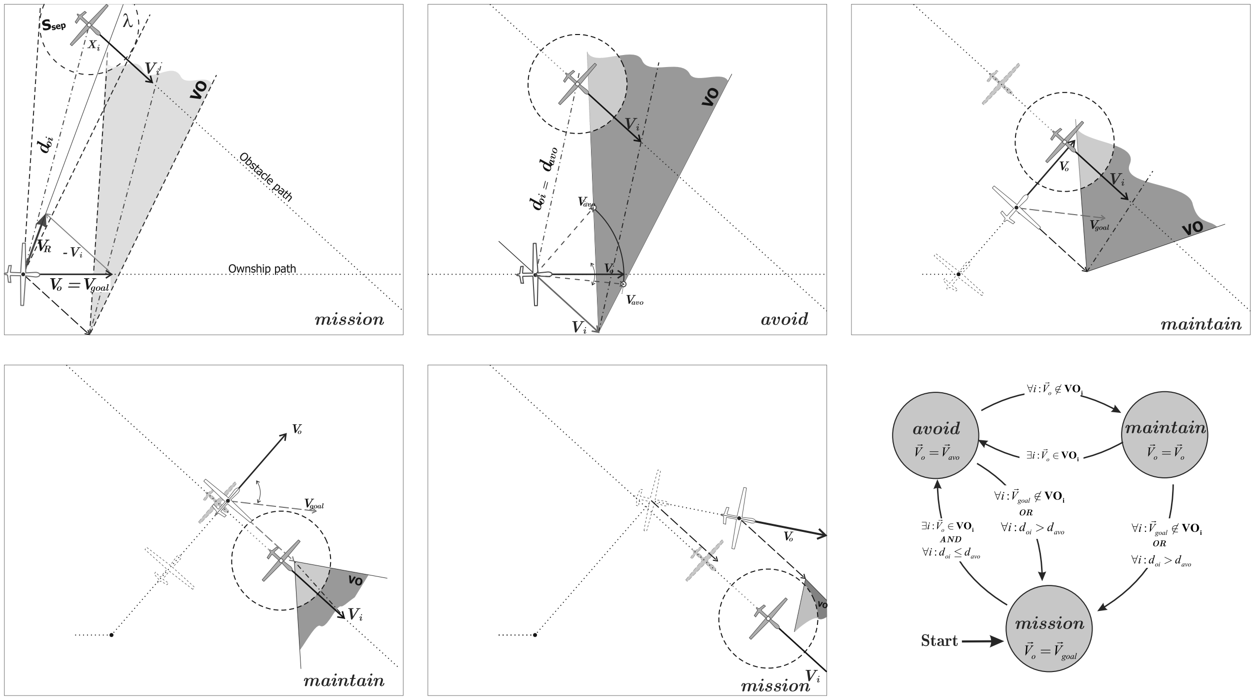

Figure 2. The Velocity Obstacle method for an example of two-dimensional encounter case

$$v_{a_y}^2 + v_{a_x}^2 = \left|\vec{V}_o\right|^2 \tag{9}$$

where the coefficient m_{vo} in equation (8) represents the two edges of the VO set, presented in equation (10) for both left and right turning directions. To ensure the existence of solutions in a circumstance when the avoidance have to be conducted inside the separation zone, the term $\left(d_{avo}^2 - r_{sep}^2\right)$ is set to be zero whenever $d_{avo} < r_{sep}$. This particular case might occur when a avoidance failed due to dynamic interaction of the vehicles. Hence the resolution changes from separation maintaining to separation regaining, to direct the vehicle to leave the separation zone as fast as possible.

$$m_{vo} = -\frac{\delta_\chi x_i^* r_{sep} + y_i^* \sqrt{d_{avo}^2 - r_{sep}^2} - d_{avo} v_{i_y}^*}{x_i^* \sqrt{d_{avo}^2 - r_{sep}^2} - \delta_\chi y_i^* r_{sep} - d_{avo} v_{i_x}^*}, \qquad \begin{cases} \delta_\chi = 1 & \text{, for left turning} \\ \delta_\chi = -1 & \text{, for right turning} \end{cases} \tag{10}$$

The V_{avo} for both direction are chosen from the set of V_a solution that have at most two real members, which are the two closest solution from the current V_o, satisfying the argument in equation (11).

$$V_{avo} = \begin{cases} \left\{ V_a \middle| \left(v_{a_x}, v_{a_y}\right) \in \mathbb{R}, \frac{v_{a_y}}{v_{a_x}} > 0, \min\left(\frac{v_{a_y}}{v_{a_x}}\right) \right\} & \text{, for left turning} \\ \left\{ V_a \middle| \left(v_{a_x}, v_{a_y}\right) \in \mathbb{R}, \frac{v_{a_y}}{v_{a_x}} < 0, \min\left(-\frac{v_{a_y}}{v_{a_x}}\right) \right\} & \text{, for right turning} \end{cases} \tag{11}$$

The variation of resolution is produced by alternating the distance where the avoidance started (d_{avo}), and the radius of the separation zone (r_{sep}). The former parameter affects the aggressiveness of the resolution: the closer the avoidance starting point from the obstacle, the more aggressive the maneuver will be. On the other hand, the radius of the separation zone, under the state diagram in Figure 2, is exactly the closest point of approach (CPA) between the vehicles. Example of conflict resolution variation can be observed in Figure 3, which is simulated with assumption of instantaneous change of velocity in one time step.

Hence, the parameters d_{avo} and r_{sep} are uniformly randomized between a specified range to create a heterogeneous situation in an integrated airspace with variety of resolution maneuver. The avoidance starts between 10 and 100 meters, which direct the vehicles to avoid other with CPA between 5 and 25 meters.

This is a self-archived version. Please find the completed version of this paper at http://arc.aiaa.org/doi/10.2514/6.2016-1000 (doi:10.2514/6.2016-1000)

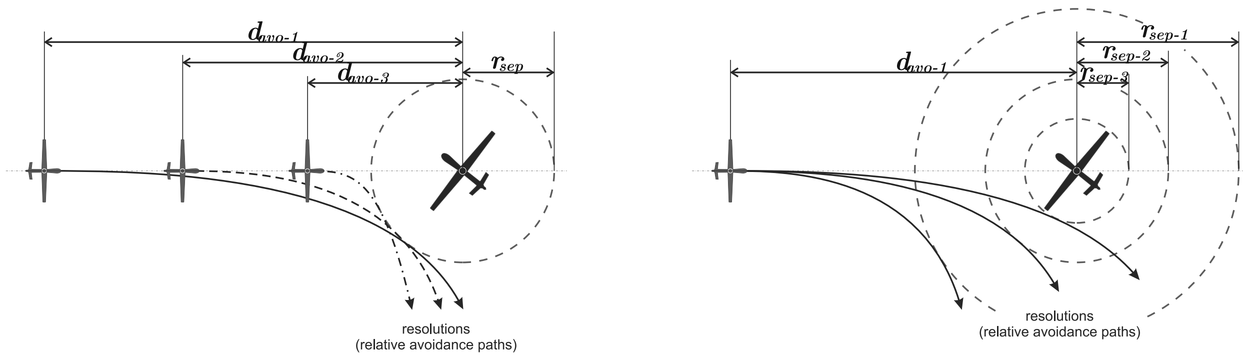

(a) (b)

Figure 3. Example of resolutions varieties due to different preferences of (a) avoidance starting distance (d_{avo}) and (b) Separation radius (r_{sep})

III. Monte Carlo Simulation Results

Figure 4 shows examples of the Monte Carlo simulations for three different density, using time-captures from a top-down point-of-view of the area of interest. Each circle in the frames represents the NMAC separation circles for each vehicle with 50 meter of radius, while the line extending from the center of the circle represent the velocity vector of each vehicle.

Four vehicles in the center of the areas are shaded and drawn with a dashed track-line to show examples of vehicle motions in following mission, avoiding, and maintaining. The initial headings of these four are especially set in the direction of the four edges of the area. Note that the time step for each density case is different in order to present sufficient flight-paths and the effects of the PBC setup. The simulation time length for each density case is chosen to ensure that every vehicle have crosses the edge of the area of interest at least once, which is the time required for the lower limit of the vehicle speed to cover the area diagonal.

As expected, it is more difficult for the vehicles to stay in its intended path in the denser airspace. Nevertheless, no body collision is recorded during the simulation, even though many NMAC occurs. This mean that while separation is violated, the vehicles still can find a path for avoidance and for going back to the mission. Figure 4 demonstrates this with the four center vehicles. On the densest airspace in Figure 4-a, two of the four are able to reach the edge of the Area of interest after some struggle to avoid collisions.

When the airspace is less dense as shown in Figure 4-b, All four center vehicles are able to reach the edge. It is interesting to note that while using the same avoidance algorithm, the drifts are much larger in the less dense airspace, which shows that the vehicles are able to find a resolution path by exploiting the empty space around them. In the densest airspace, on the other hand, the drift is suppressed since the conflicts are resolved before an appropriate resolution path is found. Instead, the vehicles mostly violate the NMAC during the avoidance process and, therefore, the conflict eventually fade due to the difference of direction.

In the least dense airspace in Figure 4-c, one of the center vehciles actually is able to complete its path to the edge, without needed to conduct any avoidance. One other vehicle only requires a small drift, while the other two require relatively large drift of drifting. This results shows the less risk of conflicts in a less dense airspace, even when the vehicles are heterogeneous. Nevertheless, some UAVs are still required to make a large avoidance, such as turning more than 180 degree, to avoid a collision.

To properly asses the safety of UAV in a heterogeneous airspace, three parameters are derived from the simulations of 1000 randomized samples for each density setup. These includes the mean ratios of time in which the vehicle is in mission, avoidance, maintain, and NMAC situation to the total operation time, or $\bar{\tau}^{mi}$, $\bar{\tau}^{av}$, $\bar{\tau}^{ma}$, and $\bar{\tau}^{\text{NMAC}}$ respectively. These parameters are defined for each airspace sample in equation (12). Here, the term **mode** referred to the corresponding time parameters of each vehicle-j in the simulation sample-i is in either mission (mi), avoidance (av), maintain (ma), or in an NMAC (NMAC) situation. N_v is the total number of vehicles of each airspace sample j which is simulated for T_j second.

This is a self-archived version. Please find the completed version of this paper at http://arc.aiaa.org/doi/10.2514/6.2016-1000 (doi:10.2514/6.2016-1000)

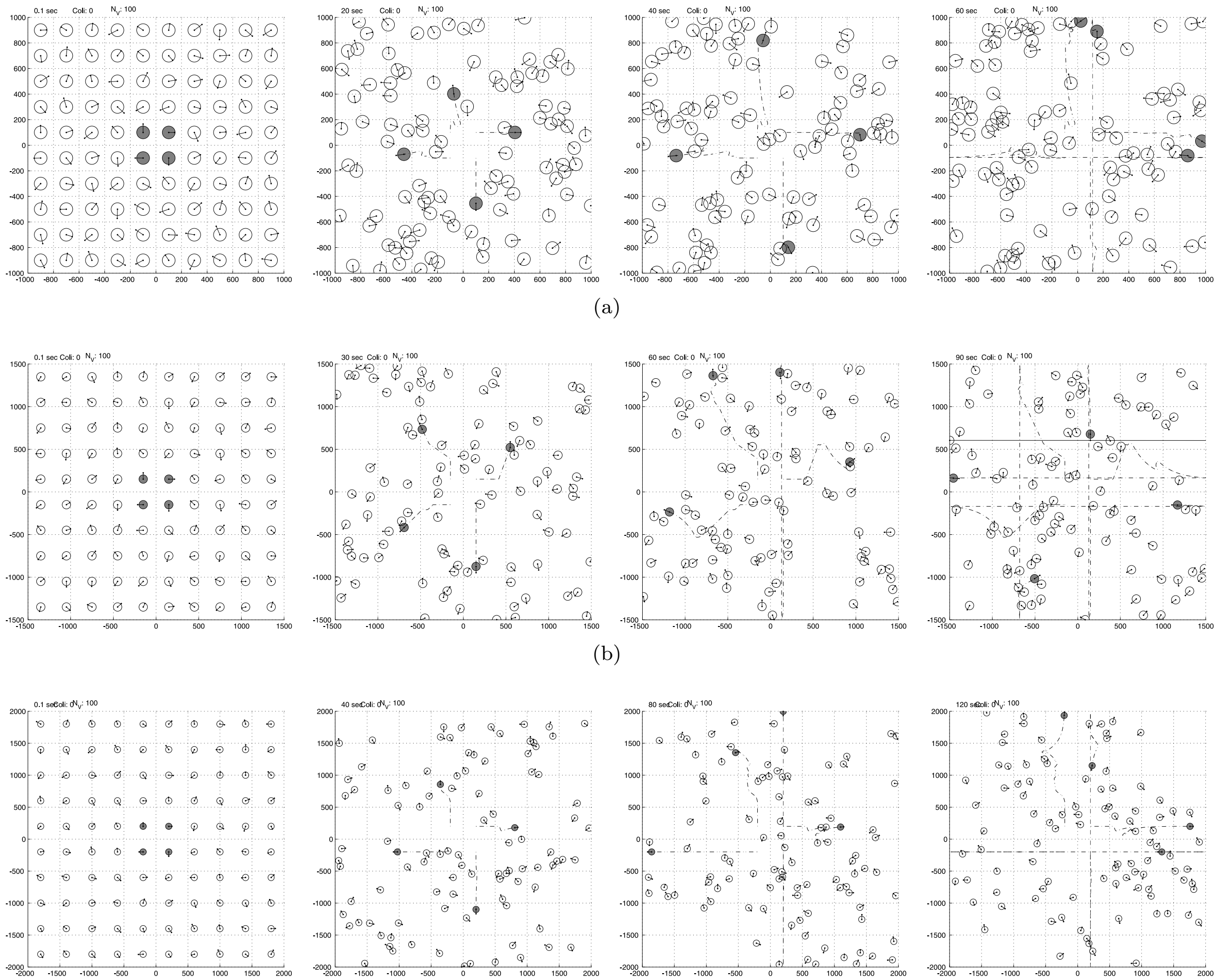

(a) (b) (c)

Figure 4. Example of the High-Density airspace simulation for three different airspace density

$$\bar{\tau}_j^{\text{mode}} = \frac{1}{N_v} \sum_{i=1}^{N_v} \frac{t_i^{\text{mode}}}{T_j} \tag{12}$$

The expected value of those time parameters is therefore approximated using their averages across the Monte Carlo airspace samples-$j = 1, 2, ..., N_{MC}$, as it is presented in equation (13). Notice that these parameters, $\bar{\tau}^{\text{mode}}$, have also already been averaged in equation (12) across the 100 vehicles in each sample. The parameter variances are estimated in the Monte Carlo simulation, using equation

$$E\left[\bar{\tau}^{\text{mode}}\right] = \frac{1}{N_{MC}} \sum_{j=1}^{N_{MC}} \bar{\tau}_j^{\text{mode}} \tag{13}$$

$$\sigma_{\bar{\tau}}^2\big|_{\text{mode}} = \frac{1}{N_{MC}-1} \sum_{j=1}^{N_{MC}} \left(\bar{\tau}_j^{\text{mode}} - E\left[\bar{\tau}^{\text{mode}}\right]\right)^2 \tag{14}$$

Finally, the precision of the Monte Carlo estimation is concluded using the central limit theory, resulting the parameter to be within the range presented in equation (15), for 99.95% confidence interval.

$$\bar{\tau}^{\text{mode}} = \left[E\left[\bar{\tau}^{\text{mode}}\right] - \frac{3.3\ \sigma_{\bar{\tau}}\big|_{\text{mode}}}{\sqrt{N_{MC}}}, E\left[\bar{\tau}^{\text{mode}}\right] + \frac{3.3\ \sigma_{\bar{\tau}}\big|_{\text{mode}}}{\sqrt{N_{MC}}}\right] \tag{15}$$

This is a self-archived version. Please find the completed version of this paper at http://arc.aiaa.org/doi/10.2514/6.2016-1000 (doi:10.2514/6.2016-1000)

The overall result of the time parameter derivation is listed in Table 2. An example of the parameters derivation in shown in the $\bar{\tau}_{\mathrm{NMAC}}$ convergence graph in Figure 5. The parameter converges quickly after approximately 50 airspace samples, demonstrate the effectiveness of the simulation setup in generating sufficient samples of random conflicts encounters and resolutions. The shaded background on each plot in Figure 5 represent the corresponding 99.95% confidence interval.

Table 2. Results of the Parameter for Safety Assessment

Mean Time of	Symbol	Results (99.95% confidence)		
		$\rho = 25/km^2$	$\rho = 11.11/km^2$	$\rho = 6.25/km^2$
NMAC, without CD&R	$\bar{\tau}^{\mathrm{NMAC}}$	$20.87 \pm 0.61\%$	$11.34 \pm 0.59\%$	$7.35 \pm 0.54\%$
NMAC, with CD&R	$\bar{\tau}^{\mathrm{NMAC}}$	$2.61 \pm 0.30\%$	$1.08 \pm 0.13\%$	$0.30 \pm 0.04\%$
Modes during operation with CD&R,				
Mission Mode	$\bar{\tau}^{mi}$	$51.27 \pm 0.75\%$	$67.77 \pm 0.52\%$	$75.76 \pm 0.41\%$
Avoid Mode	$\bar{\tau}^{ma}$	$30.05 \pm 1.19\%$	$10.77 \pm 0.45\%$	$5.33 \pm 0.17\%$
Maintain Mode	$\bar{\tau}^{av}$	$18.57 \pm 0.56\%$	$21.40 \pm 0.35\%$	$18.89 \pm 0.34\%$

Figure 5 compares cases where no avoidance implemented and cases where CD&R is activated. The result for the first case is basically the chance of NMAC occurrence in the airspace. The result shows that the CD&R implementation are able to reduce the NMAC occurrence, however not to the level expected, especially on the cases with $25/km^2$ density that leaves more than $2.61 \pm 0.30\%$ chance of NMAC. Even in the least dense airspace of the simulations, the use of CD&R system cannot guaranteed the safety, while they actually demonstrate a reduction from $7.35 \pm 0.54\%$ to only $0.30 \pm 0.04\%$ chance of NMAC.

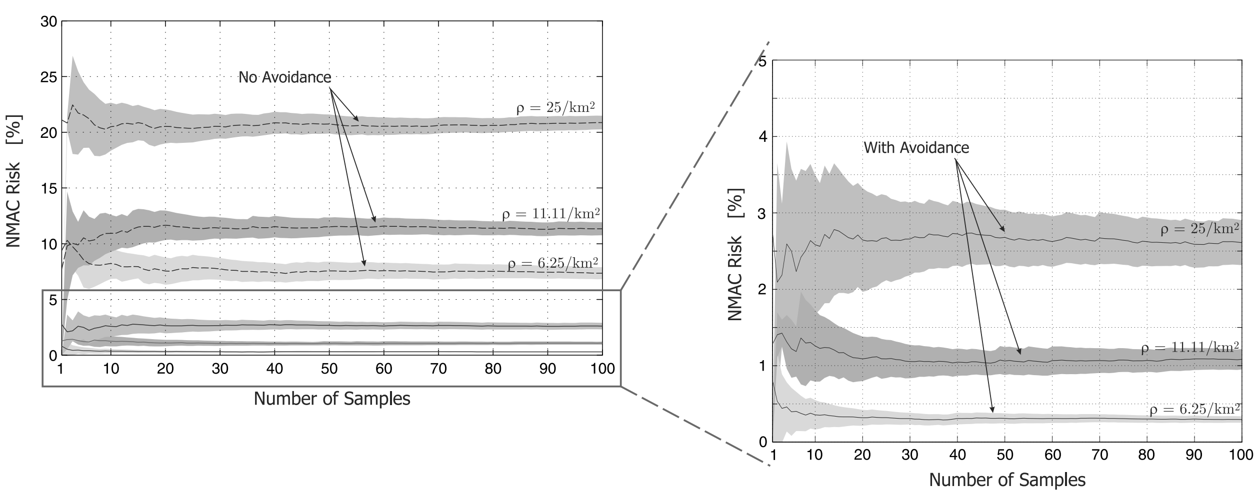

Figure 5. Monte Carlo simulation results for the Mean Time of NMAC, for case without and with CD&R (inset)

Figure 7 shows the three mean-time parameters, on operations with the CD&R in a heterogeneous airspace, in a bar graph for easier comparisons. Evidently, the mean-time when the UAVs are able to perform their mission increases as the density of the airspace decreases. In the highest density of 25 vehicle per kilometer square, the time to perform the mission is almost the same with the time to avoid. In this high density setup, the results even shows that from the avoidance performed, most of the time the vehicle is in avoidance mode, meaning that it change its direction, trying to find a resolution path, around 30% of the time. this is also have been shown before, that on this density, the algorithm actually does not find a resolution and instead, the conflict fade by it self due to the direction difference. Other density setup shows the domination of maintain mode, in which the vehicle is directed to a specific resolution path.

Table 3 shows another simulation setup, with a level of maneuver coordination by forcing every vehicle to avoid by turning to the right. This setup intended to eliminates the problem of reciprocating dance, where

This is a self-archived version. Please find the completed version of this paper at http://arc.aiaa.org/doi/10.2514/6.2016-1000 (doi:10.2514/6.2016-1000)

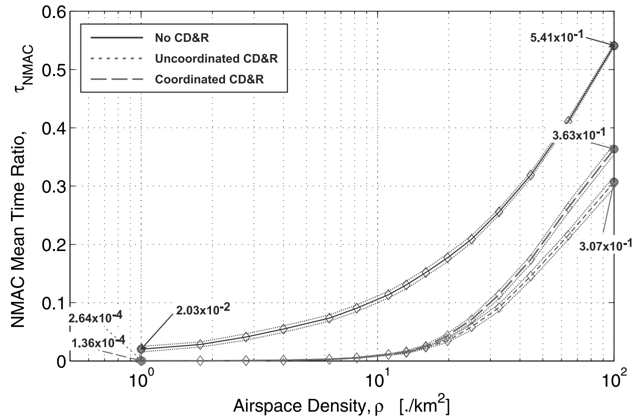

Figure 6. Mdododo

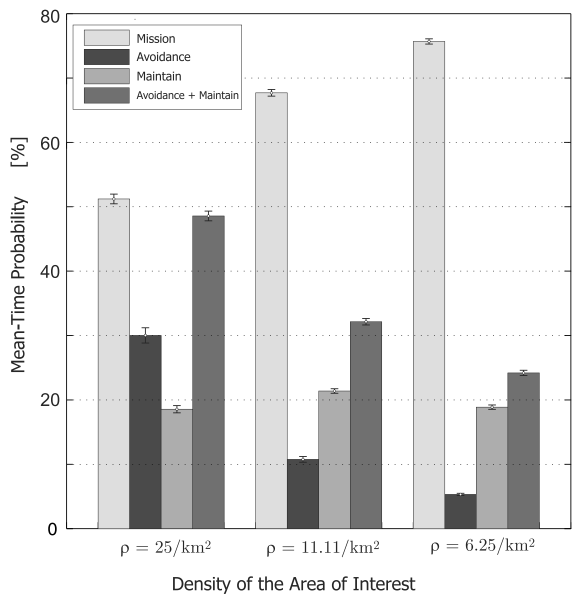

Figure 7. Mean-time parameters results for operation with CD&R in heterogeneous airspace, in three different density

a pair of vehicle avoid each other to the same side, which caused a new conflict. Coordinating by turning to the right is also a part of the Visual Flight Rule (VFR)[13] in manned flight.

The table, however, shows an adverse result. On the high density airspace, the NMAC risk actually gets much higher, to $7.06 \pm 0.53\%$. On the less dense airspace, however, an insignificant reduction of the NMAC risk is produced. These probably happen because while the coordination eliminates the reciprocating dance on head-on encounter, it produce more dance in the taking-over maneuver, where vehicles are moving approximately in the same direction. Randomization of avoidance direction is actually benefiting, since it lower the chance of reciprocating dance in both head-on and taking over encounter, and opening more avoidance path, especially in a high density airspace.

Mean-time of mission in the coordinated airspace, however, is recorded significantly higher for all three different density. This is due to the less time it needed for each avoidance to clear the conflict, since both vehicle are avoiding in the contributing direction.

This is a self-archived version. Please find the completed version of this paper at http://arc.aiaa.org/doi/10.2514/6.2016-1000 (doi:10.2514/6.2016-1000)

Table 3. Results of the Parameter for Safety Assessment in Coordinated Airspace

Mean Time of	Symbol	Results (99.95% confidence)		
		$\rho = 25/km^2$	$\rho = 11.11/km^2$	$\rho = 6.25/km^2$
NMAC, with CD&R	$\bar{\tau}^{\mathrm{NMAC}}$	$7.06 \pm 0.53\%$	$1.07 \pm 0.11\%$	$0.28 \pm 0.04\%$
Modes during operation with CD&R,				
Mission Mode	$\bar{\tau}^{mi}$	$55.66 \pm 0.75\%$	$72.85 \pm 0.42\%$	$80.00 \pm 0.40\%$
Avoid Mode	$\bar{\tau}^{ma}$	$28.23 \pm 0.99\%$	$9.16 \pm 0.33\%$	$4.26 \pm 0.14\%$
Maintain Mode	$\bar{\tau}^{av}$	$16.02 \pm 0.38\%$	$17.99 \pm 0.32\%$	$15.70 \pm 0.34\%$

IV. Conclusion

This paper has assessed the safety of Unmanned Aerial Vehicles (UAVs) operation when it is integrated in the airspace system. Three parameters have been derived including the mean ratio of time in which the vehicle are in either mission mode, avoidance mode, or in a Near Mid Air Collision (NMAC) situation for three case of airspace density. It is demonstrated that Monte Carlo simulation can be used to asses the safety by simulation setup of high density airspace, coupled with the the use of periodic boundary conditions.

While the method is able to assess the safety in various operation condition in an integrated airspace, several limitations are noted. The method has not been demonstrated in a Three-dimensional setup, while the two-dimensional is more stressful. Nevertheless, the proposed method is a versatile safety assessment method for various encounter situations a UAV might face in its operation in an integrated airspace system.

References

[1]Dalamagkidis, K., Valavanis, K. P., and Piegl, L. A., "On Integrating Unmanned Aircraft Systems into the National Airspace System," *International Series on Intelligent Systems, Control, and Automation: Science and Engineering*, Vol. 36, Springer Science+Business Media, 1st ed., 2009, doi: 10.1007/978-94-007-2479-2.

[2]Reich, P. G., "Analysis of Long-Range Air Traffic Systems: Separation Standards I," *The Journal of Navigation*, Vol. 50, 9 1997, pp. 436–447, doi:10.1017/S0373463300019068.

[3]May, G., "A Method for Predicting the Number of Near Mid-Air Collisions in a Defined Airspace," *Operational Research Quarterly (1970-1977)*, Vol. 22, No. 3, 1971, pp. 237–251, doi:10.2307/3007993.

[4]Alexander, B., "Aircraft density and midair collision," *Proceedings of the IEEE*, Vol. 58, No. 3, March 1970, pp. 377–381, doi:10.1109/PROC.1970.7643.

[5]Jenie, Y. I., van Kampen, E.-J., and Remes, B., "Cooperative Autonomous Collision Avoidance System for Unmanned Aerial Vehicle," *Advances in Aerospace Guidance, Navigation and Control*, edited by Q. Chu, B. Mulder, D. Choukroun, E.-J. Kampen, C. Visser, and G. Looye, Springer Berlin Heidelberg, 2013, pp. 387–405, doi: 10.1007/978-3-642-38253-6_24.

[6]Kochenderfer, M. J., Holland, J. E., and Chryssanthacopoulos, J. P., "Next Generation Airborne Collision Avoidance System," *Lincoln Laboratory Journal*, Vol. 19, No. 1, 2012, pp. 55–71, doi: 10.2747/1548-1603.48.1.24.

[7]Jenie, Y. I., van Kampen, E., de Visser, C. C., and Chu, Q. P., "Selective Velocity Obstacle Method for Cooperative Autonomous Collision Avoidance System for UAVs," *AIAA Guidance, Navigation, and Control Conference 2013*, AIAA, Boston, MA, 2013.

[8]Jenie, Y. I., Kampen, E.-J. v., de Visser, C. C., Ellerbroek, J., and Hoekstra, J. M., "Selective Velocity Obstacle Method for Deconflicting Maneuvers Applied to Unmanned Aerial Vehicles," *Journal of Guidance, Control, and Dynamics*, Vol. 38, No. 6, 2015, pp. 1140–1146.

[9]Mohleji, S. C. and Wang, G., "Modeling ADS-B Position and Velocity Errors for Airborne Merging and Spacing in Interval Management Application," *Technical Paper*, The MITRE Corporation, 2010.

[10]Kuchar, J. and Yang, L., "A Review of Conflict Detection and Resolution Modeling Methods," *Intelligent Transportation Systems, IEEE Transactions on*, Vol. 1, No. 4, Dec 2000, pp. 179–189, doi:10.1109/6979.898217.

[11]Jenie, Y. I., van Kampen, E., Ellerbroek, J., and Hoekstra, J. M., "Conflict Detection and Resolution System Architecture for Unmanned Aerial Vehicles in Civil Airspace," *AIAA Infotech @ Aerospace, AIAA Scitech Conference 2015*, AIAA, Kissimmee, FL, 2015, AIAA 2015-0483, doi:10.2514/6.2015-0483.

[12]Fiorini, P. and Shiller, Z., "Motion Planning in Dynamic Environments Using Velocity Obstacles," *The International Journal of Robotics Research*, Vol. 17, No. 7, 1998, pp. 760–772, doi: 10.1177/027836499801700706.

[13]Federal Aviation Administration, *Federal Aviation Regulations (FAR) Chapter I, subchapter F Air Traffic and General Operating Rules, Section 91.113 Right-of-way rules: Except water operations*.

This is a self-archived version. Please find the completed version of this paper at http://arc.aiaa.org/doi/10.2514/6.2016-1000 (doi:10.2514/6.2016-1000)